Tanzania Journal of Engineering and Technology 2024, **43**(1):144-157
OPEN ACCESS articles distributed under Creative Commons Attribution Licence [CC BY-ND]
Websites: https://ajol.org/tjet; https://tjet.udsm.ac.tz

ISSN 1821-536X (**print**); ISSN 2619-8789 (**electronic**)
https://doi.org/10.52339/tjet.v43i1.986

Regular Research Manuscript

Effect of Zr and W Doping on Microstructures, Transition Temperature and Solar Transmittance Modulation of Thermochromic W/Zr Co-Doped VO_2 Thin Films

Haji. F. Haji[1,2†], Nuru. R. Mlyuka[1], Margaret. E. Samiji[1]

[1]Physics Department, University of Dar es Salaam, P.O. Box 35063, Dar es Salaam, Tanzania.
[2]Department of Natural Sciences, The State University of Zanzibar, P. O. Box 146, Zanzibar, Tanzania.
[†]Corresponding author: haji.faki@suza.ac.tz

ABSTRACT

Thermochromic W/Zr co-doped VO_2-based thin films with different concentrations of Zr were successfully deposited on soda lime glass substrates by direct current (DC) magnetron sputtering of V(99)W(01) alloy and Zr targets at a substrate temperature of 425 °C. The films were characterized by x–ray diffraction (XRD), atomic force microscopy (AFM), Rutherford backscattering spectroscopy (RBS), two-point probe and UV/VIS/NIR spectroscopy. The film's structural properties evolution was significantly influenced by Zr concentration in the films. The transition temperature and hysteresis loop widths of the films were found to decrease with increasing Zr concentration. For the Zr concentrations of 0.21 at.%, 0.23 at.% and 0.36 at.% the films' transition temperatures were 38.1°C, 35.7 °C and 33.7 °C, respectively, whereas the corresponding hysteresis widths were 12.9 °C, 5.7 °C and 2.6 °C. Films with 0.36 at.% Zr demonstrated a high value of solar transmittance modulation at 8%, albeit with some compromise in luminous transmittance. These results reveal that a controlled amount of Zr in the W-doped VO_2 films can potentially improve the films' thermochromic properties for smart Windows applications.

ARTICLE INFO
Submitted: **Dec. 23, 2023**
Revised: **March 11, 2024**
Accepted: **May, 27, 2024**
Published: **June, 2024**

Keywords: W/Zr co-doped VO_2, Transition Temperature, Thermochromic Properties, Rutherford backscattering Spectroscopy, hysteresis widths.

INTRODUCTION

VO_2 thin films are extensively studied for the development of energy-saving devices, particularly for smart windows (Haji et al., 2023, Mlyuka *et al.*, 2009). These films exhibit a first-order structural phase change near 68 °C, which occurs rapidly (Kang *et al.*,2018, Shen *et al.*, 2014, Xu *et al.*, 2019, Haji *et al.*, 2023). The phase change in VO_2 films is accompanied by significant changes in the electrical and optical properties of the films (Azad *et al.*, 2022). For VO_2 films to be used in smart windows, several limitations that hinder large-scale production of VO_2-based thin films need to be addressed (Xu *et al.*, 2019). These limitations include high transition temperature (τ_c), low luminous transmittance (T_{lum}) and limited solar transmittance modulation (ΔT_{sol}) (Li et al. 2012, Li *et al.*, 2013). To overcome these challenges, it is recommended that τ_c is lowered to near room temperature, T_{lum} and

ΔT_{sol} are improved to above 40% and 10%, respectively (Granqvist, 2013).

Various approaches have been explored to reduce τ_c and improve both T_{lum} and ΔT_{sol} of VO_2-based thin films. These approaches include the use of multilayer structures, elemental doping, structural modifications, and the use of different substrates (Wang *et al.*, 2016). Among these, elemental doping has shown promising results in enhancing the thermochromic properties of VO_2-based thin films (Shao *et al.*, 2018). Several dopants have been investigated and demonstrated significant effects on the thermochromic behavior of VO_2 films, including W (Duo *et al.*, 2018, Liu *et al.*, 2016), Mo (Phoempoon and Sikongo 2016, Mai *et al.*, 2006), Ca (Dietrich *et al.*, 2015), Zn (Jiang *et al.*, 2014), Nb (Batista *et al.*, 2011, Piccirillo *et al.*, 2007), Mg (Mlyuka *et al.*, 2010, Li *et al.*, 2013, Gagaoudakis *et al.*, 2016, Panagopoulou *et al.*, 2016), F (Dai *et al.*, 2013) and Al (Lyobha *et al.*, 2018). Among these dopants, W doping has been found to have the most significant impact on reducing τ_c to ~ 28 °C in VO_2-based thin films (Hu *et al.*, 2016). However, it has been reported that W doping compromises both T_{lum} and ΔT_{sol} of VO_2 films (Huang *et al.*, 2020, Mlyuka, 2010). One potential solution is to combine W doping with other dopants such as Zn, Mg, Zr, Al, Tb, and Eu that have been shown to have a positive effect on T_{lum} and ΔT_{sol} of VO_2-based thin films (Cao et al. 2019, Jiang *et al.*, 2014, Wang *et al.*, 2015). Dopant combinations, such as W and Al, have shown improvements in both T_{lum} and ΔT_{sol} of VO_2 films; however, an increase in Al doping concentration was found to raise τ_c (Lyobha *et al.*, 2018). Additionally, co-doping of W and Mg in VO_2 films improved both T_{lum} and τ_c but the reduction in τ_c need further improvements (Wang *et al.*, 2015). Recently, the effect of W and Zn co-doping of VO_2-based thin films, demonstrating promising results in terms of improvements in both T_{lum} and τ_c was reported (Haji *et al.*, 2023). Incorporating Zn into VO_2 thin films can significantly impact their morphology, leading to reduced grain sizes and enhanced optical transmittance (Laurenti *et al.*, 2017). However, precisely controlling the oxygen partial pressure during deposition in the presence of Zn remains challenging, as it can promote the formation of ZnO in the structure (Cui *et al.*, 2018). While ZnO formation may improve transmittance, it can also reduce a yellowish colour to the VO_2-based thin films. This discoloration might negatively affect the thermochromic properties of the films, which are crucial for their application in energy-efficient smart windows. Therefore, in this work, we report on the results of the investigation into the influence of W and Zr co-doping of VO_2-based thin films with different concentrations of Zr. This is due to prior observation that Zr, could decrease τ_c, increase the T_{lum} along with improvements of ΔT_{sol}, as well as modifying the colour of the VO_2-based thin films (Shen *et al.*, 2014).

METHODS AND MATERIALS

EXPERIMENTAL DETAILS

Preparation of W/Zr Co-doped VO_2

W/Zr co-doped VO_2 thin films were fabricated on soda lime glass substrates by reactive DC magnetron sputtering of 99.9% pure Zr and V(99)W(01) at.% alloy targets both supplied by Plasmaterials Company (2268 Research Drive, Livermore, CA 94550-USA). The supplied targets had a dimension of 2-inch diameter by 0.250-inch thick. Argon (99.999%) and oxygen (99.9%) were employed as sputtering and reactive gases, at flow rates of 75 ml/min and 4.32 ml/min, respectively. A base pressure of 9.4×10^{-6} mbar and a working pressure of 4.7×10^{-3} mbar were maintained. The substrate temperature was set at 425 °C and the sputtering power for V(99)W(01) target was 120 W while that for Zr target was varied between 10 to 20 W to obtain different doping levels. The substrate temperature was maintained at

above 400 °C as its promotes the formation of well crystallized structure of the VO_2-based thin films (Maodong et al.2018). The configuration of the sputtering system utilized in this work is depicted in Figure1. The substrate inside the vacuum chamber of the coating unit shown in Figure 1 was heated by a radiant heater that was installed just above it. The substrate temperature was controlled, as per calibration curve presented elsewhere (Haji, 2024), by adjusting the voltage to the heater filament between 0 and 240 V in 10 V increments using variac transformer. The temperature at the bottom of the substrate was measured after the system reached a stable temperature, which took about 60 minutes for each voltage setting. The film's thickness of ~ 96 nm was estimated based on the deposition rates, which was later confirmed using a Tencor Alpha step IQ surface profiler with stylus force of 15.6 mg. The transmittance values of the W/Zr co-doped VO_2 thin films were determined using a Perkin Elmer 1050+ UV/VIS/NIR Spectrophotometer. The integrated luminous and solar transmittance values of the films were calculated from spectral transmittance data using Equation (1) (Mlyuka et al., 2009, Haji et al., 2023).

$$T_{lum,sol} = \frac{\int \Phi_{lum,sol}(\lambda) T(\lambda) d\lambda}{\int \Phi_{lum,sol}(\lambda) d\lambda} \qquad (1)$$

where $T(\lambda)$ is transmittance, Φ_{lum} is the standard luminous efficiency function for the photonic vision of human eyes ($380\ nm \le \lambda \le 760\ nm$), and Φ_{sol} is the solar irradiance spectrum for air mass 1.5 (corresponding to the sun standing 37 ^{o} above the horizon). Solar modulation ΔT_{sol} is obtained as $\Delta T_{sol} = T_{sol,25\,^oC} - T_{sol,100\,^oC}$.

Characterization of W/Zr Co-doped VO_2

The temperature-dependent sheet resistance of the W/Zr co-doped VO_2 thin films was determined using a two-point probe (TPP). To determine the switching characteristics of the films, the electrical and optical measurements were conducted. At the same time the sample temperature was varied from 25 °C to 100 °C and back for heating and cooling cycles, respectively. X-ray diffraction (XRD) analysis was performed on the W/Zr co-doped VO_2 samples to identify the VO_2 phases present in the films. Cu K-Alpha x-ray radiation with wavelength of 0.1504 nm was used in continuous scanning measurement mode with 2θ scanning range of 5° to 80°. Additionally, the average crystallite sizes and lattice micro-strain (ε) of the films were estimated using the Williamson-Hall formula equation (2), which involved a linear fit of the plots of $4\sin\theta$ against $\beta\cos\theta$ (Ollotu *et al.*, 2020, Haji *et al.*, 2023).

$$\beta\cos\theta = 4\varepsilon\sin\theta + \frac{k\lambda}{D} \qquad (2)$$

where β is the full width at half maximum, θ is Bragg's diffraction angle, D is the crystallite size, k is the scatter constant estimated to be 0.94 for spherical crystallites, and λ is the x-ray radiation wavelength. The surface morphology of the films was characterized using the Digital Instruments Nanoscope (R) IIIa multimode Atomic Force Microscope (AFM) operating in tapping mode. AFM images of the samples were obtained with a scan rate of 1.960 Hz and a scan size of 1.00 μm. Subsequently, the AFM images were analyzed using Gwydion and WSxM software to determine the grain size distribution and roughness parameters (Ollotu *et at.*, 2020). The elemental concentrations of the W/Zr co-doped VO_2 thin films were determined through Rutherford backscattering spectroscopy (RBS). RBS measurements took place through the bombardment of the samples by alpha particles ^4He (2+) at a pressure of 10^{-5} mbar and accelerating energy of 2.80 MeV and scattering angle of 150^o (Figure 2). Determination of concentration of dopants was achieved by fitting the

experimental and simulated RBS spectral data using

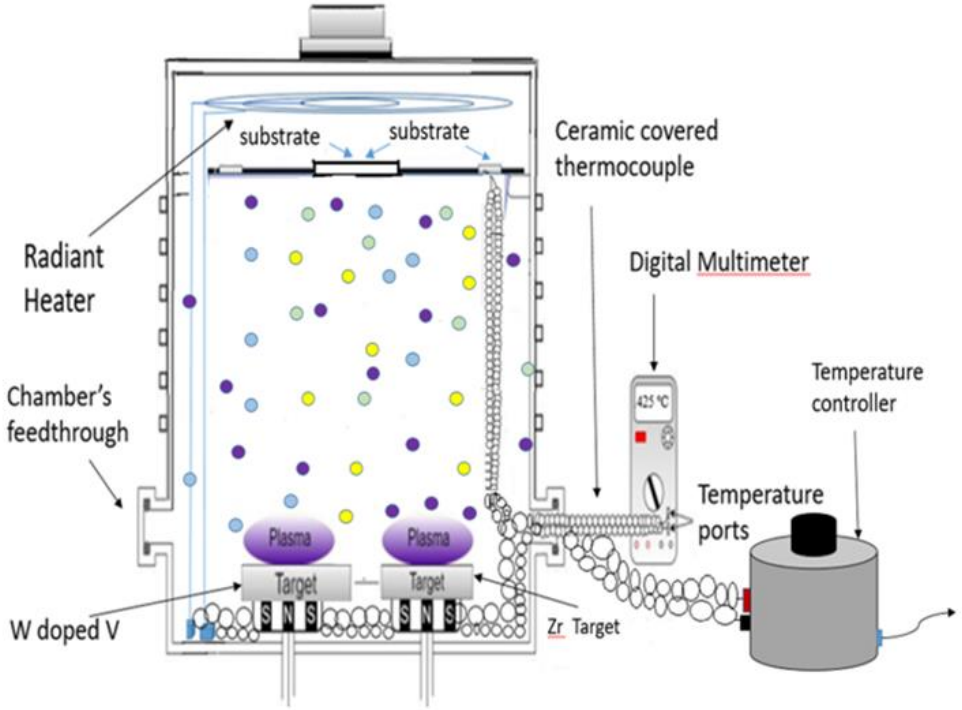

Figure 1: Schematic diagram of the sputtering chamber with thermocouples connected to the outside temperature controller and digital multi-meter through the chamber's feedthrough (Haji *et al.*, 2023).

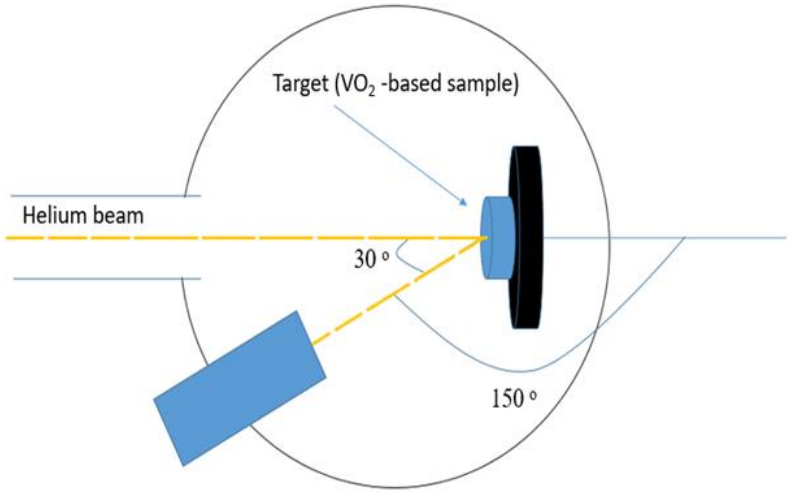

Figure 2: Schematic diagram for the Rutherford backscattering spectroscopy measurements to determine the elemental composition in the samples using alpha particles ^{4}He (2+).

RESULTS AND DISCUSSION

X-Ray Diffraction Analysis

Figure 3 displays the XRD patterns of W/Zr co-doped VO_2 thin films with different Zr doping levels. For all samples, prominent diffraction peaks were observed at 2θ values of 27.86°, 39.76°, 44.68°, 56.84°, and 72.037° that correspond to the (0 1 1), (0 0 2), (0 1 2), $(1\ 1\ \overline{3})$, and $(4\ 1\ \overline{1})$ miller indices, respectively, of the monoclinic VO_2 based on the reference datasheet PDF # 44 - 0253. The plots of 4Sinθ against

βCosθ obtained from the Williamson-Hall formula (Equation 2) and their linear fits for W/Zr co-doped VO_2 thin films with different Zr concentrations are shown in Figure 4 a, b and c. Data from these plots were used to extract crystallite sizes and lattice micro-strains of the films shown in Figure 4 d. The Figure reveals that crystallite sizes of W/Zr co-doped VO_2 thin films decrease with increasing Zr concentration, where 0.21 at.% Zr concentration exhibits crystallite sizes of ~ 6.9 nm while that of 0.36 at.% Zr concentration was ~ 3.4 nm. A Similar trend was observed for the lattice micro-strain of the films. It should be noted that micro-strain affects the stability of metallic phases in the VO_2-based thin films (Haji et al. 2023). The strain reduction observed due to Zr doping has the potential to improve the stability of the metallic phase and reduce the transition temperature of VO_2-based thin film. The combination of W and Zr dopants provides the ability to tailor the transition temperature of VO_2-based thin films, and higher Zr concentrations may even enable the reduction of the transition temperature below room temperature.

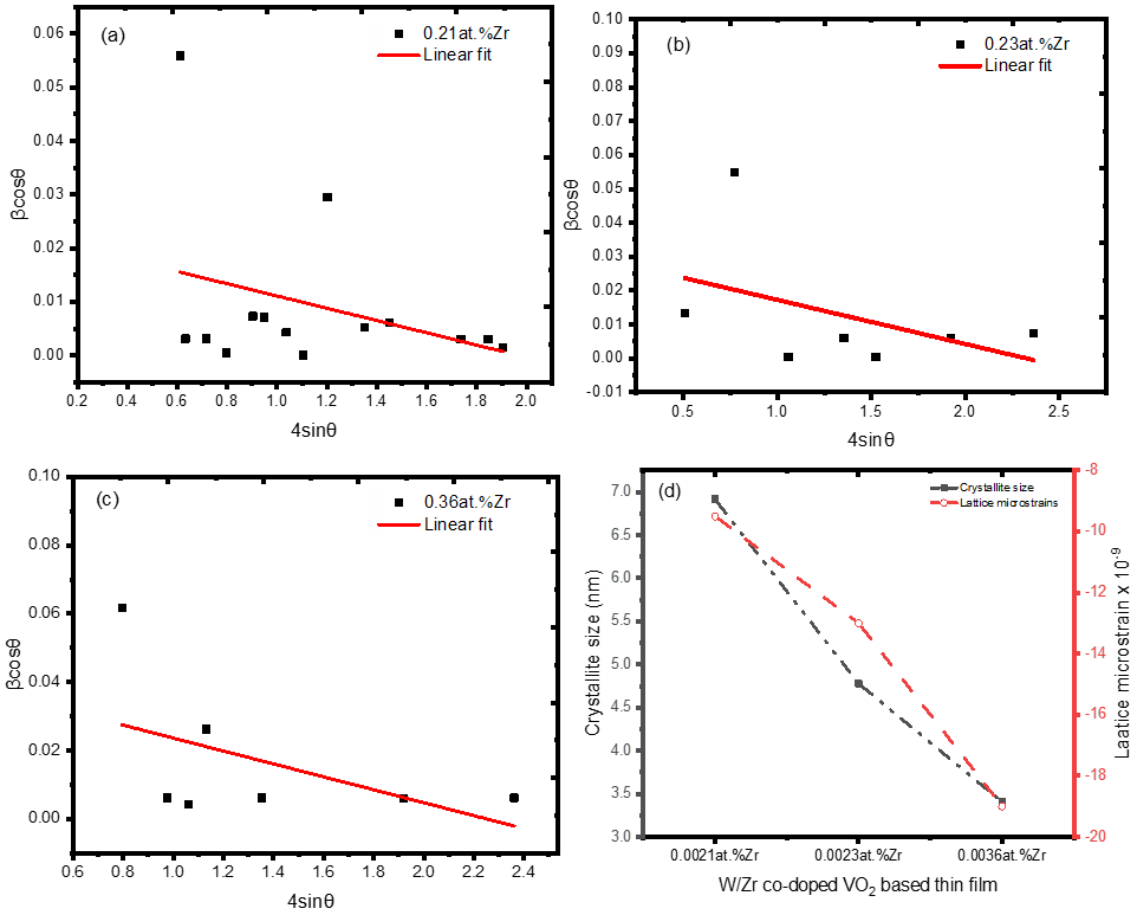

Figure 4: Plots of βCosθ against 4Sinθ, from the Williamson – Hall formula for the W/Zr co-doped VO_2 based thin films, (a) ~ 0.21 at.% Zr, (b) ~ 0.23 at.% Zr, (c) ~ 0.36 at.% Zr and (d) their corresponding average crystallite sizes and micro strains.

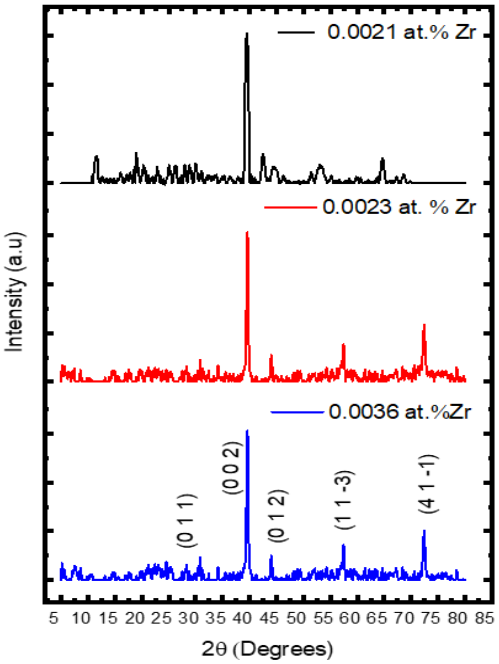

Figure 3: XRD pattern of W/Zr co-doped VO_2 thin films for different Zr doping levels.

Atomic Force Microscopy Analysis

Fig. 5 illustrates three-dimensional AFM images of W/Zr co-doped VO_2 films, along with their corresponding grain size distribution, depict small, roundish and uniformly distributed grains. The uniformity and small size of grains in VO_2 films can improve their thermochromic properties, making them suitable for smart coatings and textiles that change colour with temperature variation (Gorobtsov et al., 2022). As can be observed in Table 1, the root mean square roughness, R_{rms} of the W/Zr co-doped VO_2-based thin films decreased with increasing Zr concentrations in the samples, with R_{rms} = 23 for ~ 0.21 at.% Zr, whereas R_{rms} = 9 for films containing ~ 0.36 at.% Zr. The reasons for this trend in grain size and RMS could not be ascertained from our data, but literature suggest that W and Zr doping can fill vacancies or interstitials sites in VO_2 crystal lattice leading to a smoother surface and consequently lowers RMS (Kuo *et al.*, 2007). Table 1 further reveals that increasing the concentration of Zr in the W/Zr co-doped VO_2 thin films leads to a decrease in both the average and maximum heights of the grains. These results are consistent with the X-ray diffraction (XRD) measurements, as depicted in Figure 3, where the crystallite sizes decrease with increasing Zr concentration in the W/Zr co-doped VO_2 thin films. The reduction in grain size is likely attributed to the higher level of Zr doping, which increases the number of grain boundaries, and consequently lowers the τ_c and narrows the hysteresis loop width of the W/Zr co-doped VO_2-based thin film. This suggests a τ_c in the vicinity of room temperature and a more accurate switching between insulating and metallic states of W/Zr co-doped VO_2 thin films for smart windows (Yannick *et al.*, 2023). Additionally, the observed grain size reduction in AFM data might also reduce the light scattering and absorption, which might enhance the NIR transmittance (Figure 9) of the VO_2-based thin films.

Table 1 Statistical parameters analyzed from AFM measurements of W/Zr co-doped VO_2-based thin films

Sample Name	RMS roughness (R_{rms})	Mean roughness (R_a)	Average height (nm)	Maximum height (nm)
VO_2:W:Zr (0.21 at.% Zr)	23	18	54	144
VO_2:W:Zr (0.23 at.% Zr)	11	9	37	74
VO_2:W:Zr (0.36 at.% Zr)	9	7	33	69

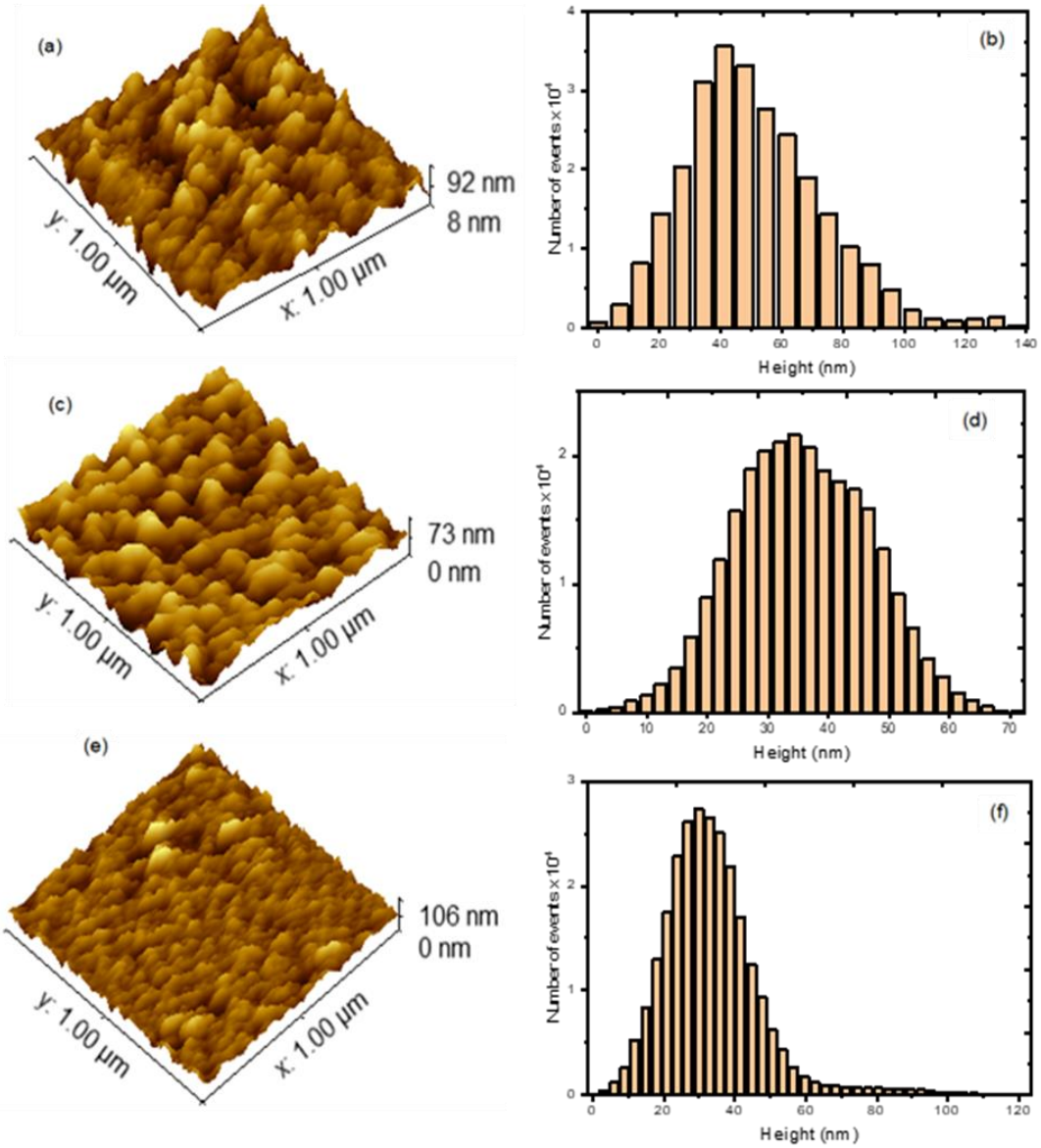

Figure 5: The 3D AFM images with corresponding grain size distributions for W/Zr co-doped VO_2-based thin films with ~ 0.21 at. % Zr (a, b), ~ 0.23 at.% Zr (c, d) and ~ 0.36 at.% Zr (e, f) dopants concentrations.

Rutherford Backscattering Spectroscopy Analysis

The RBS spectra of W/Zr co-doped VO_2-based thin films with their corresponding SIMNRA simulated spectra are shown in Figure 6. A good spectral fit was observed when a maximum number of iterations of about 50 were achieved with fit accuracy value of 0.01. All the spectra in Figure 6 confirmed the presence of V, O, Si, W and Zr peaks. Si peaks likely originated from soda lime glass substrates used in this work while other elements are from the W/Zr co-doped VO_2-based thin films. The W dopant concentration was controlled at ~ 0.95 at.% for all films and the influence of Zr dopant concentrations on thermochromic properties of W/Zr co-doped VO_2 films was determined. Figure 6 (a) shows RBS spectra of W/Zr co-doped VO_2 thin films with different Zr concentrations realised by the Zr target's varying sputtering power. The Zr concertation in the samples was determined to be ~ 0.21at.%, ~ 0.23 at.%, and ~ 0.36 at.%, for Zr target sputtering

powers of 10 W, 15 W and 20 W, respectively. Thus, a slight change in Zr concentration of the W/Zr co-doped VO_2-based thin films possesses a significant change in the thermochromics properties of VO_2 films as will be discussed in the sections 3.4 and 4.5. Variation of dopant concentration with depth for W/Zr co-doped VO_2 thin film is shown in Fig. 7. The Figure shows uniform doping levels for W and Zr across the depth of the films and nearly the same film thickness for all samples. The oxygen atoms were found to be nearly twice the concentration of vanadium atoms in all samples as can be observed from the depth profile presented in Figure 7. This is due to stoichiometric composition of VO_2 in VO_2 based crystal structure, where by each vanadium atom is bonded to possible six oxygen atoms, forming a distorted octahedral coordination (Liu *et al.*, 2018). However, the vanadium peak looks sharp and strong than other elements in the RBS spectra, due to its higher atomic number, Z =23 compared to that of Si substrate (Z=14). Havier elements scatter more strongly resulting in a more pronounced signals in the RBS spectrum (Gracia-Hemme *et al.*, 2017).

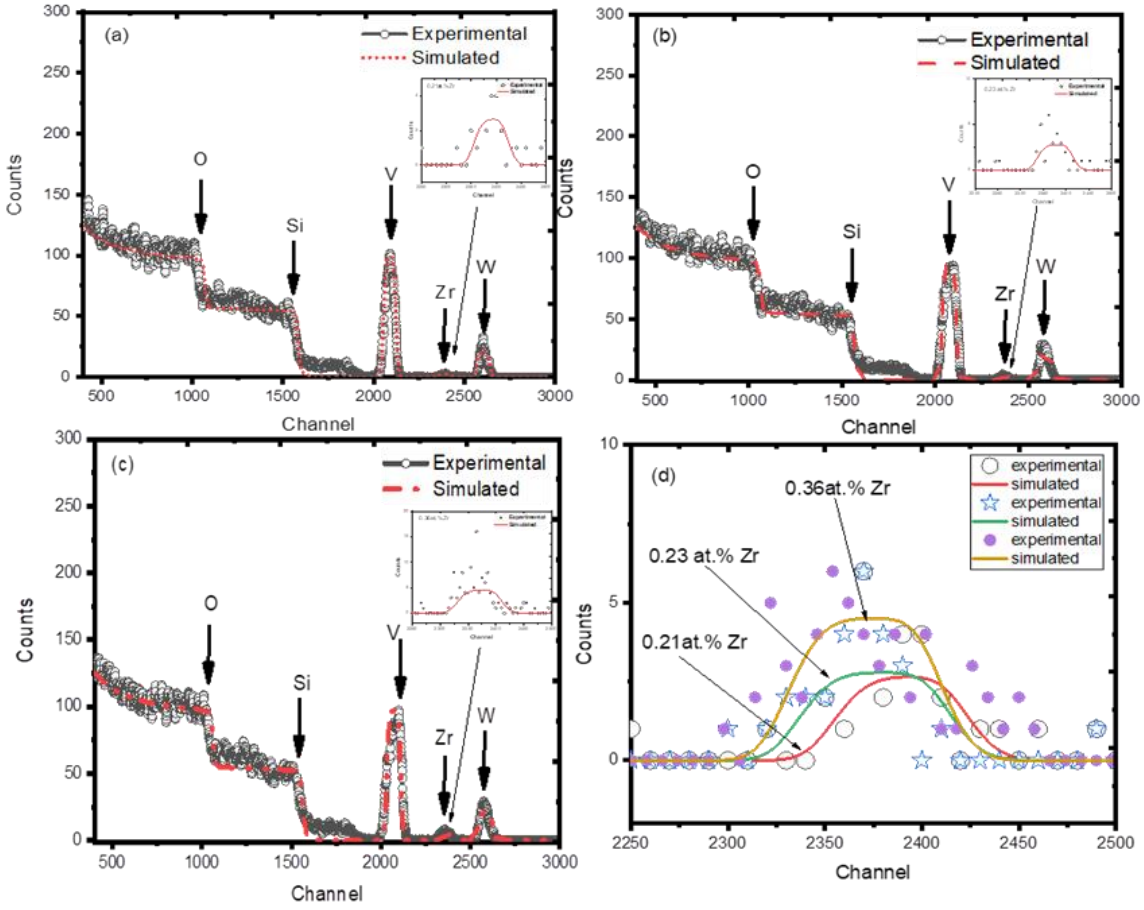

Figure 6 (a), (b), (c) RBS data with SIMNRA spectra of VO_2:W: Zr thin films for different Zr sputtering powers and doping levels and (d) Enlarged spectra for the concentration of Zr in W/Zr co-doped VO_2 thin films

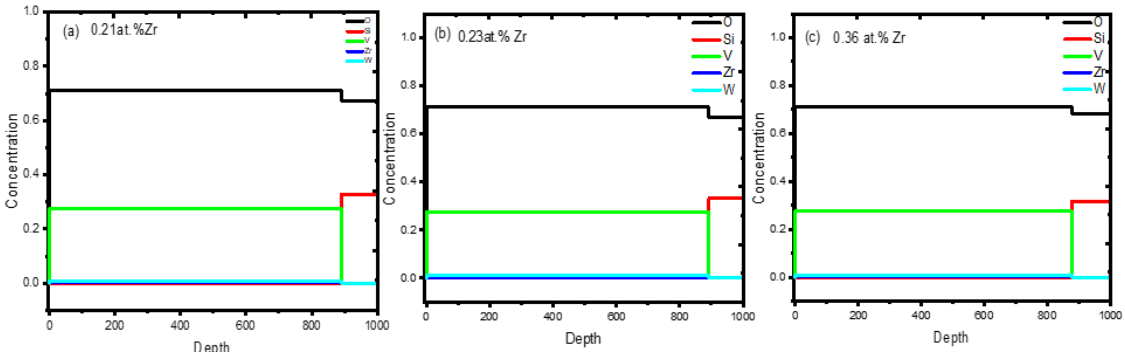

Figure 7: Depth profile for the dopants concentration in W/Zr co-doped VO_2 based thin films deposited onto soda lime glass substrates.

Electrical Properties of W/Zr co-doped VO_2 based thin films

The variation of natural logarithms of resistance as a function of temperature for the W/Zr co-doped VO_2-based thin films is presented in Figure 8 (a), (b) and (c), and their corresponding transition temperature values displayed in Figure 8 (d). Sheet resistance of W/Zr co-doped VO_2 thin films was found to decrease with increasing Zr doping levels in the samples with R_s = 1.5 x 10^7 Ω, 1.23 x 10^7 Ω and 1.89 x 10^6 Ω for films with ~0.23 at.% Zr and ~0.36 at.% Zr respectively in the semiconducting state. A similar trend was observed for the metallic state of the films. The τ_c values were determined from the average of the minimum derivatives of the temperature dependence of resistance for heating and cooling curves as has been done by other authors (Mlyuka, 2010). Inserts in Figure 8 (a), (b) and (c) are the resistance vs temperature differential curves versus temperatures for the W/Zr co-doped VO_2-based thin films. These inserts were also used to determine the hysteresis loop width of the films as well as τ_c. The hysteresis loop widths were found to decrease with increasing Zr dopant concentration. In particular, films with ~ 0.21 at.% Zr showed relatively wide hysteresis loop of about 12.9 °C compared to 5.7 °C and 2.6 °C for films with ~ 0.23 at.% Zr and ~ 0.36 at.% Zr, respectively. VO_2-based thin films with ~ 0.21 at.% Zr was determined to have τ_c of ~38.1 °C whereas that for the films with ~ 0.23 at.% Zr and ~ 0.36 at.% Zr were determined to be 35.7 °C and 33.7 °C, respectively (Figure 8 d).

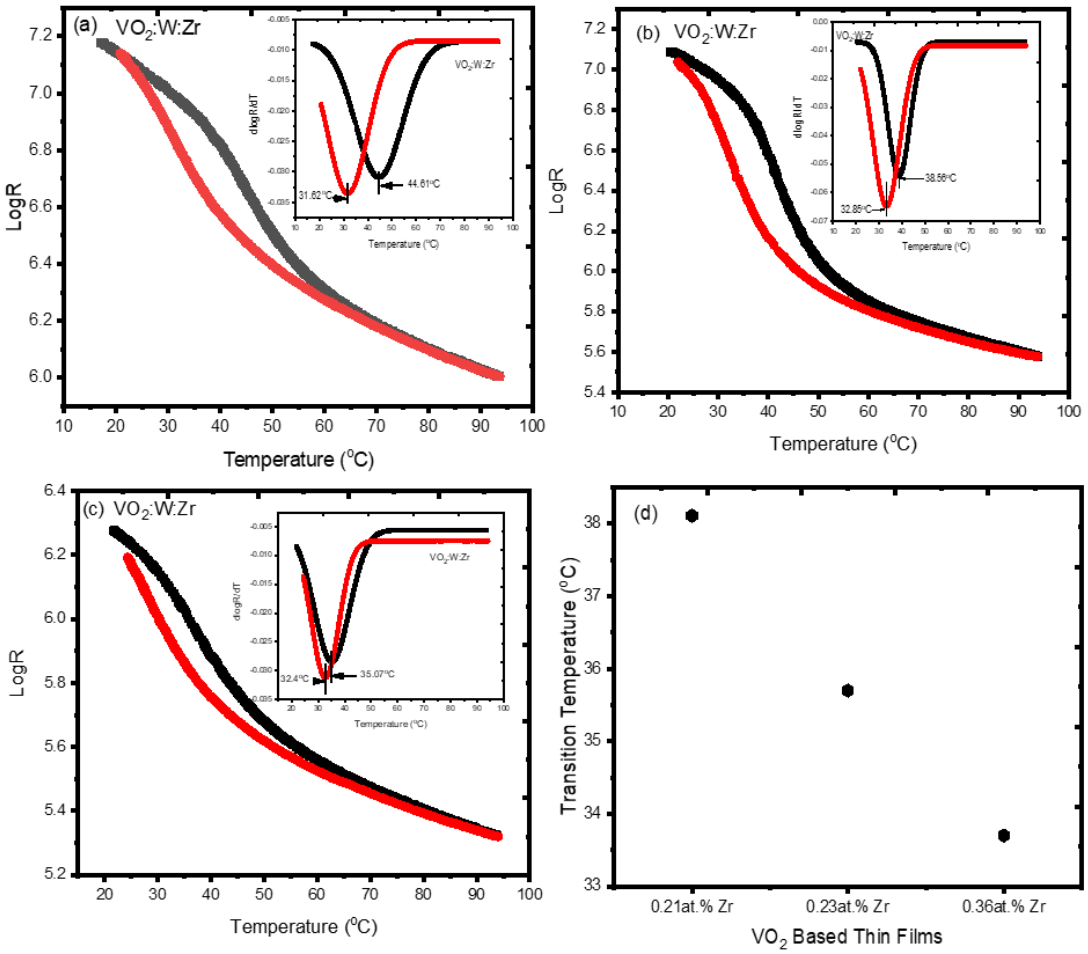

Figure 8: Temperature dependence of resistance for W/Zr co-doped VO_2 based thin films with different Zr dopants concentrations; (a) 0.21 at.% Zr, (b) 0.23 at.% Zr, (c) 0.36 at.% Zr, and (d) corresponding transition temperatures.

Optical Properties of W/Zr co-doped VO_2-based thin films

The spectral transmittance for semiconducting ($T < \tau_c$) and metallic phases ($T > \tau_c$) of W/Zr co-doped VO_2 thin films with different Zr doping concentrations are presented in Figure 9. The peak transmittance of ~ 46% was observed in the visible spectral range at a wavelength, λ = 614 nm. It was also observed that near-infrared transmittance modulation, ΔT at λ = 2000 nm, a wavelength with maximum contrast in transmittance of the films, was observed to be ~22.96%, ~34.32% and ~57.11% for the films with ~ 0.21 at.% Zr, ~ 0.23 at.% Zr and ~ 0.36 at.% Zr, respectively. The integrated luminous and solar transmittance as well as solar transmittance modulation were investigated to evaluate the potentials of W/Zr co-doped VO_2-based thin films in smart window applications and the results are summarized in Table 2. W/Zr co-doped VO_2 films with 0.21 at.% Zr possessed a relatively large value of T_{lum} at about 48.4% compared to 36.4% and 31.8% for the films with 0.23 at.% Zr and 0.36 at.% Zr, respectively. On the other hand, the integrated solar transmittance modulation of W/Zr co-doped VO_2 thin films was found to increase with increasing Zr dopant concertation. Thin films with 0.36 at.% Zr possessed a relatively large value of ΔT_{sol} at 8% compared to 2% for the films with 0.21 at.% Zr (Table 2).

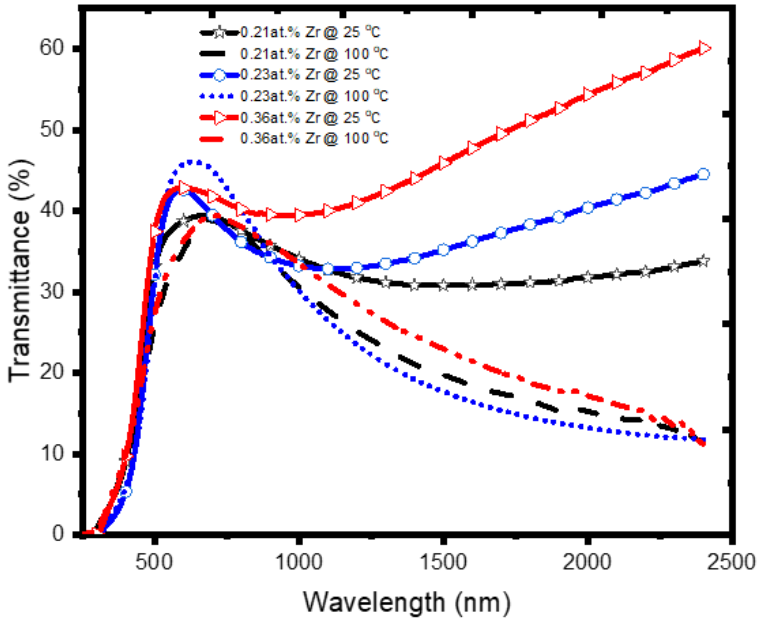

Figure 9: Spectral transmittance for W/Zr co-doped VO_2 thin films with different doping levels of Zr at 25 ° C and 100 ° C,

Table 2 Variation of Luminous, T_{lum} and Solar Transmittances, T_{sol} for W/Zr co-doped VO_2 thin films

Sample	$T_{lum,\ 25^oC}$ (%)	$T_{lum,\ 100^oC}$ (%)	$T_{sol,\ 25^oC}$ (%)	$T_{sol,\ 100^oC}$(%)	ΔT_{sol} (%)
VO_2:W:Zr (0.21 at.% Zr)	47.1	48.4	48.0	46.0	2.0
VO_2:W:Zr (0.23 at.% Zr)	38.0	36.4	32.8	30.7	2.1
VO_2:W:Zr (0.36 at.% Zr)	37.1	31.8	37.3	29.4	8.0

CONCLUSION AND RECOMMENDATIONS

The W/Zr co-doped VO_2 thin films were successfully prepared by DC magnetron sputtering at a substrate temperature of 425 °C. Crystallite and grain sizes as well as film roughness were found to decrease significantly with increasing Zr concentrations. The transition temperature of the W/Zr co-doped VO_2 films was observed to decrease with increasing Zr concentration at 38.1°C, 35.7 °C and 33.7 °C for 0.21 at.% Zr, 0.23 at.% Zr, and 0.36 at.%Zr, respectively. The hysteresis width of the films was also found to decrease with increasing Zr concentration at 12.9 °C, 5.7 °C and 2.6 °C for films with ~ 0.21 at.%, 0.23 at.% and ~ 0.36 at.%, respectively. Furthermore, solar transmittance modulation, ΔT_{sol} of W/Zr co-doped VO_2 films with 0.36 at.% Zr was relatively higher at 8% compared to 2.1% and 2.0% for the films with 0.23 at.% Zr and 0.21 at.% Zr respectively. This work revealed that a controlled amount of Zr in the W-doped VO_2 thin films improved ΔT_{sol}, and τ_c, and therefore has the potential for smart window applications. As a way forward from this work, optimization of Zr doping to the W/Zr co-doped VO_2-based thin films need to be done to achieve a desired balance between τ_c, hysteresis width and ΔT_{sol} for practical applications in smart Windows.

ACKNOWLEDGEMENT

The International Science Program (ISP) of Uppsala University-Sweden, the National Research Foundation (NRF) iThemba LABS, and the University of Dar es Salaam (UDSM) are acknowledged for research facilities and materials. HFH is grateful to the Ministry of Education Science and Technology (MoEST) Tanzania and The State University of Zanzibar (SUZA) for PhD scholarship and study leave, respectively.

REFERENCES

Azad S, Gajula D, Sapkota N, Rao A, and Koley G 2022 Infrared Transmission Characteristics of Phase Transitioning VO_2 on Various Substrates. Micromachines (Basel). 13(5):812. https://doi.org/10.3390/mi13050812

Batista C, Carneiro J, Ribeiro RM and Teixeira V 2011 Reactive pulsed-DC sputtered Nb-doped VO_2 coatings for smart thermochromic windows with active solar control. *J. Nanoscience and Nanotechnology*. **11**(10): 9042–9045. https://doi.org/10.1166/jnn.2011.3486.

Cao X, Jin P and Luo H 2019 VO_2-based thermochromic materials and applications: flexible foils and coated glass for energy efficiency. In: *Nanotechnology in Eco-efficient Construction*. pp. 503–524. https://doi.org/10.1016/B978-0-08-102641-0.00021-9

Cui Y, Ke Y, Liu C, Chen Z, Wang N, Zhang L, and Long Y 2018 Thermochromic VO_2 for energy-efficient smart windows. Joule, 2(9), 1707-1746. https://doi.org/10.1016/j.joule.2018.06.018.

Dai L, Chen S, Liu J, Gao Y, Zhou J, Chen Z, Cao C, Luo H and Kanehira M 2013 F-doped VO_2 nanoparticles for thermochromic energy-saving foils with modified color and enhanced solar-heat shielding ability. J. *Phy. Chem. Chem. Physics.* 15: 11723–11729.https://doi.org/10.1039/C3CP51359A.

Dou S, Zhang W, Wang Y, Tian Y, Wang Y, Zhang X, Zhang L, Wang L, Zhao J and Li Y 2018 A facile method for the preparation of W-doped VO_2 films with lowered phase transition temperature, narrowed hysteresis loops and excellent cycle stability. *Mater. Chem. Phys.* **215**: 91–98. https://doi.org/10.1016/j.matchemphys.2018.05.018.

Gagaoudakis E, Kortidis I, Michail G, Tsagaraki K, Binas V, Kiriakidis G and Aperathitis E 2016 Study of low temperature rf-sputtered Mg-doped vanadium dioxide thermochromic films deposited on low-emissivity substrates. *Thin Solid Films* **601**: 99–105. https://doi.org/10.1016/j.tsf.2015.11.007.

Garcia-Hemme E, García G, Palacios P, Montero D, García-Hernansanz R, Gonzalez-Diaz G, and Wahnon P 2017 Vanadium supersaturated silicon system: a theoretical and experimental approach. Journal of Physics D: Applied Physics, 50(49), 495101. DOI 10.1088/1361-6463/aa9360.

Granqvist, C. G 2013 Chromogenic windows. In Advances in Science and Technology. Trans Tech. Publication Ltd. Vol.77. pp. 108-117.

Haji HF, Numan N, Madiba IG, Mabakachaba B, Mtshali C, Khumalo Z, Kotsedi L, Mlyuka N, Samiji M and Maaza M 2023 Zn and W Co-doped VO_2-Based Thin Films Prepared by DC Magnetron Sputtering: Improved Luminous Transmittance and Reduced Transition Temperature. *J. Electron. Mater*. **52**, 4020–4029. https://doi.org/10.1007/s11664-023-10382-1.

Haji HF, Numan N, Madiba IG, Samiji ME, Mlyuka NR, and Maaza M 2023 Zr and W Co-doped VO_2 thin films with improved luminous transmittance and transition temperature. Journal of Materials Science: Materials in Electronics, 34(30), 2006. DOI https://doi.org/10.1007/s10854-023-11381-y.

Haji HF, Samiji M E, and Mlyuka NR 2023 Impact of Zn and W Doping Levels on Properties of Thermochromic VO_2-Based Thin Films. Tanzania Journal of

Science, 49(4), 809-818. DOI: 10.4314/tjs.v49i4.3.

Haji HF 2024 Investigation of the Effects of Co-doping, and Multilayer Structures, on the Thermochromic Properties of Vanadium Dioxide Based Thin Films for Smart Windows Applications. PhD thesis, University of Dar es Salaam.

Hu L, Tao H, Chen G, Pan R, Wan M, Xiong D and Zhao X 2016 Porous W-doped VO_2 films with simultaneously enhanced visible transparency and thermochromic properties. J. Sol-Gel Sci. Technol. 77: 85–93. DOI https://doi.org/10.1007/s10971-015-3832-z.

Huang Z, Wu Z, Ji C, Dai J, Xiang Z, Wang D, Dong X and Jiang Y 2020 Improvement of phase transition properties of magnetron sputtered W-doped VO_2 films by post-annealing approach. *J. Mater. Sci. Mater. Electron.* **31** (5): 4150–4160. DOI https://doi.org/10.1007/s10854-020-02964-0.

Jiang M, Bao S, Cao X, Li Y, Li S, Zhou H, Luo H and Jin P 2014 Improved luminous transmittance and diminished yellow color in VO_2 energy efficient smart thin films by Zn doping *Ceram. Int.* 40: 6331–6334. https://doi.org/10.1016/j.ceramint.2013.10.083

Kang C, Zhang C, Yao Y, Yang Y, Zong H, Zhang L and Li M 2018 Enhanced Thermochromic Properties of Vanadium Dioxide (VO_2)/Glass Heterostructure by Inserting a Zr-Based Thin Film Metallic Glasses ($Cu_{50}Zr_{50}$) Buffer Layer. Applied Sciences. **8**(10).1751. https://doi.org/10.3390/app8101751

Kuo S T, Tuan W H, Shieh J, and Wang S F 2007 Effect of Ag on the microstructure and electrical properties of ZnO. Journal of the European Ceramic Society, 27(16), 4521-4527. https://doi.org/10.1016/j.jeurceramsoc.2007.02.215

Laurenti M, Castellino M, Perrone D, Asvarov A, Canavese G, and Chiolerio A 2017 Lead-free piezoelectrics: V^{3+} to V^{5+} ion conversion promoting the performances of V-doped Zinc Oxide. Scientific Reports, 7(1), 41957. https://doi.org/10.1038/srep41957.

Li SY, Mlyuka NR, Primetzhofer D, Hallén A, Possnert G, Niklasson GA and Granqvist CG 2013 Bandgap widening in thermochromic Mg-doped VO_2 thin films: Quantitative data based on optical absorption. *Appl. Phys. Lett.* **103** (16), 161907. https://doi.org/10.1063/1.4826444.

Li SY, Niklasson GA and Granqvist CG 2012 Thermochromic fenestration with VO_2-based materials: Three challenges and how they can be met. In: *Thin Solid Films*. **520**(10), 3823-3828. https://doi.org/10.1016/j.tsf.2011.10.053.

Liu D, Cheng H, Xing X, Zhang C and Zheng W 2016 Thermochromic properties of W-doped VO_2 thin films deposited by aqueous sol-gel method for adaptive infrared stealth application. *Infrared Phys. Technol.* **77**: 339–343. https://doi.org/10.1016/j.infrared.2016.06.019.

Lyobha CJ, Mlyuka NR and Samiji ME 2018 Effects of Aluminium and Tungsten Co-Doping on the Optical Properties of VO_2 Based Thin Films. *Tanz. J. Sci.* **44** (4): 91–99.

Mai LQ, Hu B, Hu T, Chen W and Gu ED 2006. Electrical property of mo-doped VO_2 nanowire array film by melting-quenching sol-gel method. *J. Phys. Chem. B* 110 (39): 19083–19086. https://doi.org/10.1021/jp0642701

Mlyuka NR 2010 *Vanadium Dioxide Based Thin Films: Enhanced Performance for Smart Window Applications.* PhD thesis, University of Dar es Salaam.

Mlyuka NR, Niklasson GA, Granqvist CG 2009 Thermochromic multilayer films of VO_2 and TiO_2 with enhanced transmittance, Solar Energy Materials and Solar Cells, 93(9): 1685-1687. https://doi.org/10.1016/j.solmat.2009.03.021.

Ollotu ER, Nyarige JS, Mlyuka NR, Samiji ME, and Diale M 2020 Properties of ITO thin films rapid thermally annealed in different exposures of

nitrogen gas. Journal of Materials Science: Materials in Electronics, 31(19), 16406-16413. https://doi.org/10.1007/s10854-020-04192-y.

Panagopoulou M, Gagaoudakis E, Boukos N, Aperathitis E, Kiriakidis G, Tsoukalas D and Raptis YS 2016 Thermochromic performance of Mg-doped VO_2 thin films on functional substrates for glazing applications. *Sol. Energy Mater. Sol. Cells* 157: 1004–1010. https://doi.org/10.1016/j.solmat.2016.08.021.

Phoempoon P and Sikong L 2016 Synthesis of thermochromic Mo-doped VO_2 particles. In: *Materials Science Forum*. pp. 88–92. Trans Tech Publications Ltd. https://doi.org/10.4028/www.scientific.net/MSF.867.88

Piccirillo C, Binions R and Parkin IP 2007. Nb-doped VO_2 thin films prepared by aerosol-assisted chemical vapour deposition. *Eur. J. Inorg. Chem.* (25): 4050–4055. https://doi.org/10.1002/ejic.200700284.

Shao Z, Cao X, Luo H and Jin P 2018 Recent progress in the phase-transition mechanism and modulation of vanadium dioxide materials. *NPG Asia Mater.* 10(7): 581–605. https://doi.org/10.1038/s41427-018-0061-2

Shen N, Chen S, Chen Z, Liu X, Cao C, Dong B, Luo H, Liu J and Gao Y 2014 The synthesis and performance of Zr-doped and W-Zr-codoped VO_2 nanoparticles and derived flexible foils. *J. Mater. Chem. A* **2** (36): 15087–15093. DOI https://doi.org/10.1039/C4TA02880E.

Wang N, Liu S, Zeng XT, Magdassi S and Long Y 2015 Mg/W-codoped vanadium dioxide thin films with enhanced visible transmittance and low phase transition temperature. *J. Mater. Chem. C* **3** (26): 6771–6777. DOI https://doi.org/10.1039/C5TC01062D.

Wang S, Liu M, Kong L, Long Y, Jiang X and Yu A 2016 Recent progress in VO_2 smart coatings: Strategies to improve the thermochromic properties. *Prog. Mater. Sci.* ***81****,1-54. https://doi.org/10.1016/j.pmatsci.2016.03.001.*

Xu J, Wang H, Lu Z, Zhang Z, Zou Z, Yu Z, Cheng M, Liu Y and Xiong R 2019 Effect of Zr Doping on the Magnetic and Phase Transition Properties of VO_2 Powder. Nanomaterials, **9**(1). 113. https://doi.org/10.3390/nano9010113.